Hindawi Publishing Corporation
Journal of Nanomaterials
Volume 2015, Article ID 304295, 8 pages
http://dx.doi.org/10.1155/2015/304295

Research Article

Catalyst-Free Bottom-Up Synthesis of Few-Layer Hexagonal Boron Nitride Nanosheets

Shena M. Stanley, Amartya Chakrabarti, Joshua J. DeMuth, Vanessa E. Tempel, and Narayan S. Hosmane

Department of Chemistry and Biochemistry, Northern Illinois University, DeKalb, IL 60115, USA

Correspondence should be addressed to Narayan S. Hosmane; hosmane@niu.edu

Received 17 March 2015; Accepted 11 August 2015

Academic Editor: Ajayan Vinu

Copyright © 2015 Shena M. Stanley et al. This is an open access article distributed under the Creative Commons Attribution License, which permits unrestricted use, distribution, and reproduction in any medium, provided the original work is properly cited.

A novel catalyst-free methodology has been developed to prepare few-layer hexagonal boron nitride nanosheets using a bottom-up process. Scanning electron microscopy and transmission electron microscopy (both high and low resolution) exhibit evidence of less than ten layers of nanosheets with uniform dimension. X-ray diffraction pattern and other additional characterization techniques prove crystallinity and purity of the product.

1. Introduction

Due to structural similarities to graphene, hexagonal boron nitride (h-BN) nanosheets have become an extremely desirable material over the last few years. While many synthetic efforts have been made to combine these two materials for several electronic applications [1–5], recently few-layer h-BN nanosheets have been successfully developed as substrates for graphene [6–8]. Furthermore, h-BN nanosheets are useful in a number of versatile applications due to unique inherent physical properties [9–11]. h-BN exhibits excellent chemical and mechanical stability and it is thermally conductive and is electrically insulating material with a wide band gap (5-6 eV) as well. While h-BN is being used as an electrical insulator in thermally conductive materials [12], composites of h-BN have been the preferred species in aircrafts for their radiation shielding properties [13].

Although the developments of graphene and graphene composites are continuously advancing, few-layer h-BN nanostructures are comparatively less investigated due to synthetic difficulties [14]. Preparation of h-BN nanostructures involves one of the two common approaches, top-down or bottom-up. The top-down process mainly includes mechanical or chemical exfoliation of h-BN nanosheets from bulk h-BN [15–17]. Although it is one of the most common techniques currently used to produce nanomaterials on a large scale, the major disadvantage of this method is the imperfection of surface structure imparted during the process [18]. On the contrary, the bottom-up approach yields nanostructures with minimal defects and superior chemical homogeneity. Typically, chemical vapor deposition (CVD) is used as a bottom-up approach. However, the requirement of substrate and extreme reaction conditions makes this synthetic route less desirable. Involvement of catalysts in a CVD process not only restricts industrial scaling-up of the method, but also yields products with metal impurities [6, 19]. It is interesting to note a recent report in which defect-free h-BN nanocrystals were produced at 1000°C in a tube furnace [20]. Consequently, a controlled cost-effective synthetic methodology to prepare h-BN nanosheets on a large scale is warranted. To the best of our knowledge, there have been no reports to date on a bottom-up methodology that avoids catalysts altogether in producing pristine few-layer h-BN nanosheets at a significantly lower temperature.

Herein we report a bottom-up synthesis for few-layer h-BN nanosheets by an autoclave pyrolysis technique that can potentially be scaled up for industrial manufacturing purposes.

$$NH_4Cl_{(s)} + KBH_{4(s)} \xrightarrow[12-48\,h]{800^\circ C} NH_3{\cdot}BH_3 + KCl + H_2$$

$$NH_3{\cdot}BH_3 + NaN_{3(s)} \xrightarrow[12-48\,h]{800^\circ C} N_{2(g)} + [B\text{-}N]_{(s)} + NaNH_{2(s)} + 2H_{2(g)}$$

$$NH_4Cl_{(s)} + KBH_{4(s)} + NaN_{3(s)} \xrightarrow[12-48\,h]{800^\circ C} KCl_{(s)} + N_{2(g)} + [B\text{-}N]_{(s)} + NaNH_{2(s)} + 3H_{2(g)}$$

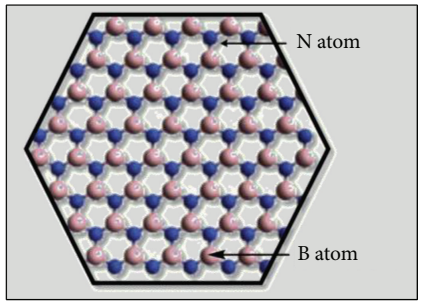

h-BNNS

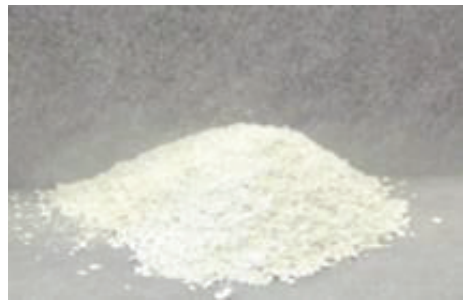

Scheme 1: Synthesis of hexagonal boron nitride nanosheets (h-BNNS).

2. Materials and Methods

All the chemicals used were from Sigma-Aldrich, KBH_4 (99.998%), NH_4Cl (99.998%), and NaN_3 (99.5%). The HCl used for purification was from Fisher Scientific. In a typical pyrolysis experiment, the reagents were assembled in an Ar glovebox containing <2.00 ppm O_2. The B and N precursors, KBH_4 (82.31 mmol), NH_4Cl (82.45 mmol), and NaN_3 (82.60 mmol), were thoroughly mixed together and transferred to a 100 mL autoclave that was sealed and then heated with varying times (12 h for BNS12, 24 h for BNS24, and 48 h for BNS48) at 800°C in a vertical furnace. After the reaction was completed, the crude product from the autoclave was washed three times with 3 M HCl with sonication between each wash. The next step was to wash with deionized water, until the pH of the decant liquid became neutral. Sonication was carried out between each water wash. The drying process included washing few times with acetone followed by evaporation of the solvent using a rotary evaporator. Finally, the purified product was dried under high vacuum at room temperature overnight.

3. Results and Discussion

The synthetic methodology involved mixing of NH_4Cl, NaN_3, and KBH_4 in equimolar proportions, in an inert atmosphere. The resulting mixture was heated at 800°C, inside a tightly closed stainless steel autoclave to produce h-BN nanosheets (Scheme 1). In order to optimize the reaction conditions and to analyze the time dependency on the morphology of the product, the pyrolysis was carried out at varied time interval of 12 to 48 h. Detailed reaction protocols are included in the supplementary information.

This innovative technique produced few-layer h-BN nanosheets with high yield in a stainless steel autoclave.

Table 1: Synthesis and electrical property of h-BN nanosheets.

Sample	Reaction conditions	Yield (%)	Band gap[a] (eV)
BNS12	800°C, 12 hrs	83	5.989
BNS24	800°C, 24 hrs	85	6.018
BNS48	800°C, 48 hrs	87	6.048

[a]Band gaps are calculated from UV-Vis spectroscopic data.

However, the exact mechanism of this process is unknown. We believe the high pressure generated during the pyrolysis facilitated the formation of few-layer nanosheets of h-BN. The advantages of this methodology over the CVD methods are manifold. While almost all of the CVD techniques require temperatures higher than 1000°C, a comparatively lower temperature, used in our synthesis, is noteworthy. In addition, the catalyst-free synthetic approach involving inexpensive starting material without the continuous stream of gas made this process unique, cost-effective, and ideal for the large scale production of this material. Nonetheless, the method is simple enough in that the rigorous purification techniques can be avoided and the products can be washed with acid and deionized water to produce pristine nanosheets. The resulting h-BN nanosheets, identified as BNS12, BNS24, and BNS48, were isolated as products from 12 h, 24 h, and 48 h reactions, respectively. The yield of the products, though in slight deviation (less than 4%), was calculated for each reaction (Table 1).

Role of the precursors in the synthesis of h-BN was also investigated systematically. The absence of NaN_3 in the equimolar mixture of KBH_4 and NH_4Cl reduced the yield of h-BN to <40% when reacted for 48 h at 800°C. On the other hand, a complete elimination of NH_4Cl from the reactant mixture failed to produce even a trace of h-BN under

identical reaction conditions indicating that all three reagents are essential components in producing h-BN nanosheets. Although the exact mechanism for the formation of h-BN in this study is not known, a plausible sequence of reaction steps, shown in Scheme 1, can be deduced based on the formation of hydrogen and nitrogen gases along with the formation KCl and water-sensitive $NaNH_2$ that were removed during the washings using 3 M HCl and deionized water. The *in situ* formation of ammonia borane ($NH_3{\cdot}BH_3$) in the first step can undergo a fast reaction with NaN_3 to produce the desired h-BN with the formation of solid $NaNH_2$ along with the formation of gaseous H_2 and N_2 as by-products. Since $NaNH_2$ is known to form an infinite polymeric tetrahedral chain, it is possible that the initial formation of the nanosheets of h-BN could occur on the surface of the $NaNH_2$ polymer.

The products were vacuum dried overnight for further characterization. Scanning electron microscopy (SEM), transmission and high resolution transmission electron microscopy (TEM and HRTEM), energy-dispersive X-ray spectroscopy (EDX), electron energy loss spectroscopy (EELS), Fourier transform infrared (FT-IR) spectroscopy, Raman spectroscopy, X-ray powder diffraction (XRD), and UV-Vis spectroscopy are the techniques used for characterizing the product.

The morphology of the BNS samples was investigated using SEM (TeScan Vega II SBH). The products were lightly coated with gold for the ease of imaging purposes. The SEM image of BNS12 exhibits uniform product dimensions (Figure 1) and the average diameter of the nanosheets was found to be approximately between 600 and 800 nm. A narrow size distribution of the products was observed for all of the samples at different time periods. Thus, we can conclude that the size of the product is independent of the reaction times.

TEM (Hitachi H-600) characterization is consistent with the findings from SEM imaging for all of the samples with product dimension falling under similar data ranges (Figures 2(a)–2(c)). On the other hand, the HRTEM (JEOL JEM-2100F) determined the number of layers of the h-BN nanosheets. While BNS12 exhibited nanosheets with an average of 6–8 layers (Figure 3(a)), BNS48 showed varied number of layers between 20 and 22 (Figure 3(b)). The spacing between the layers was estimated by measuring the thickness of the sheet and dividing it by the number of layers. The resulting value of 0.33 nm matches perfectly the previously published data [21, 22] as well as those collected *via* XRD studies. Nonetheless, the HRTEM images evidently predicted that the reaction time has a pronounced effect on the formation of h-BN layers. A controlled reaction time can reduce the number of layers without significantly changing the reaction yields.

The EDX spectra of BNS samples were generated over a large area of the products using an INCAx-act Analytical Standard EDS Detector and Figures 4(a)–4(c) depict the EDX spectra of BNS12, BNS24, and BNS48, respectively. The EDX data ascertains the elemental composition and purity of h-BN nanosheets. The atomic ratio of B : N was found to be 1 : 1 (atomic weight percentage of B : N = 50.06 : 49.94)

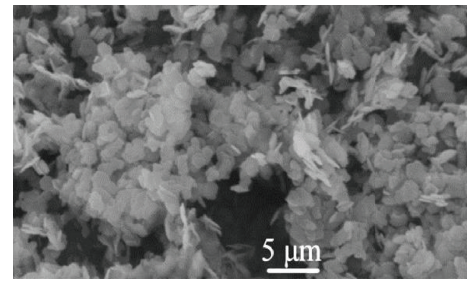

Figure 1: SEM image BNS12 showing uniform product morphology. Nanosheets of average size between 600 nm and 800 nm were observed with a narrow size distribution.

by EDX analysis. EELS data of BNS12 was obtained *via* an electron energy loss detector attached to the JEOL JEM-2100F microscope and Figure 5 represents the EEL spectrum. The peak positions and the splitting patterns in EEL spectrum confirm the sp^2 hybridization of BN in h-BN nanosheets. The energy loss around 190 eV and 400 eV corresponded to the K-shell ionization energy of the B and N atoms, respectively [23].

Bonding patterns of the B and N atoms in nanosheets and purity of the products were further verified by FT-IR (ATI Mattson Genesis Series (Figures 6(a)–6(c))) and Raman spectroscopy (Figures 7(a)–7(c)). The FT-IR peak at 1388 cm^{-1} is due to the stretching vibration of B-N bonds. A comparatively weaker peak at 815 cm^{-1} can be attributed to the bending vibration of B-N-B bonds of h-BN [24]. Raman spectroscopy of the BNS samples was performed using a Renishaw inVia Raman microscope with a 532 nm laser source. An intense sharp peak at 1364 cm^{-1} acts as the definite confirmation of the presence of h-BN in the sample [25].

The UV-visible spectroscopy (Lambda XLS+) was used to determine the UV absorption properties and the corresponding band gaps of the BNS samples (Figures 8(a)–8(c)). Very dilute and well dispersed ethanolic solutions of BNS samples were scanned between 200 and 700 nm in a quartz cell. A sharp absorption band at 207 nm (Figure 8(a)) for BNS12 reflects a band gap of 5.98 eV which is consistent with the value reported by Geick et al. for a single crystal of pure h-BN [24] A slight blue shift was noticed for BNS24 and BNS48 (Figures 8(b) and 8(c)) compared to BNS12 that can be attributed to the increasing number of layers in the nanosheets.

The XRD (Rigaku MiniFlex, Cu, 30 kV, 15 mA X-ray) patterns of the h-BN nanosheets, synthesized at 800°C, exhibited interplanar d-spacing and intensities that are indicative of h-BN crystallinity [26]. Figures 9(a)–9(c) show the spectrum of BNS12, BNS24, and BNS48, respectively, where the indexed peaks are in good agreement with the theoretical values for h-BN (JCPDS 34-0421). The lattice constants of $a = 2.508$ and $c = 6.667$ were calculated using EdPCR component of FullProf Suite software. Nonetheless, all of the XRD patterns suggest formation of highly ordered and pure h-BN nanosheets.

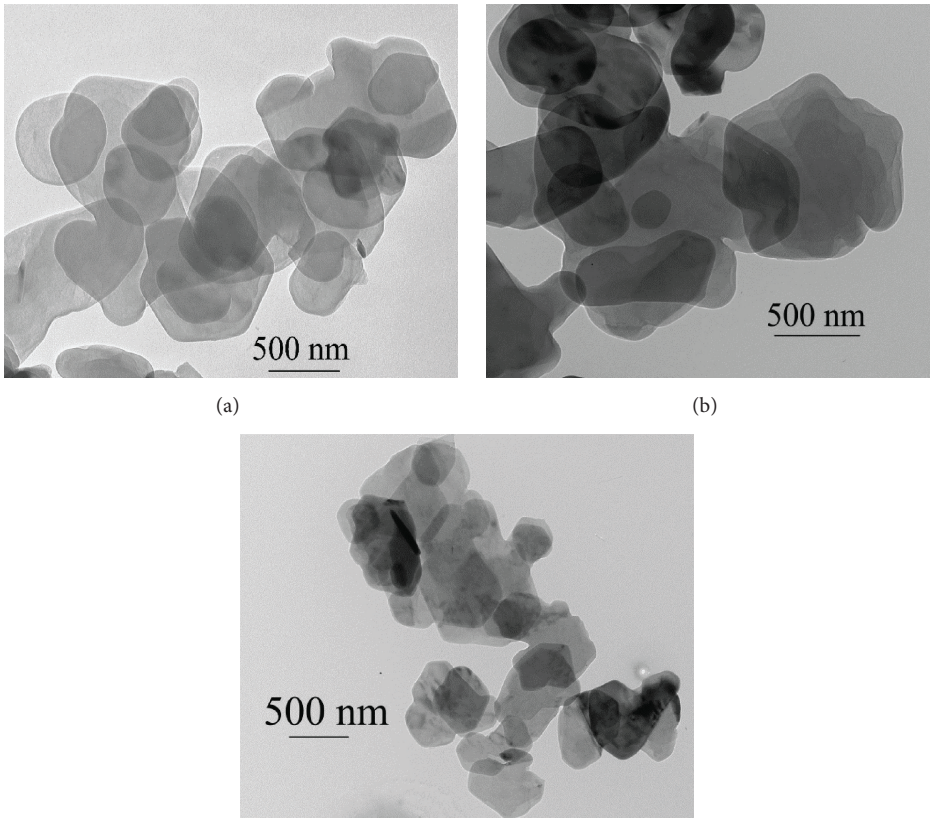

(a) (b)

(c)

Figure 2: TEM images of (a) BNS12, (b) BNS24, and (c) BNS48 exhibiting size distributions in agreement with SEM.

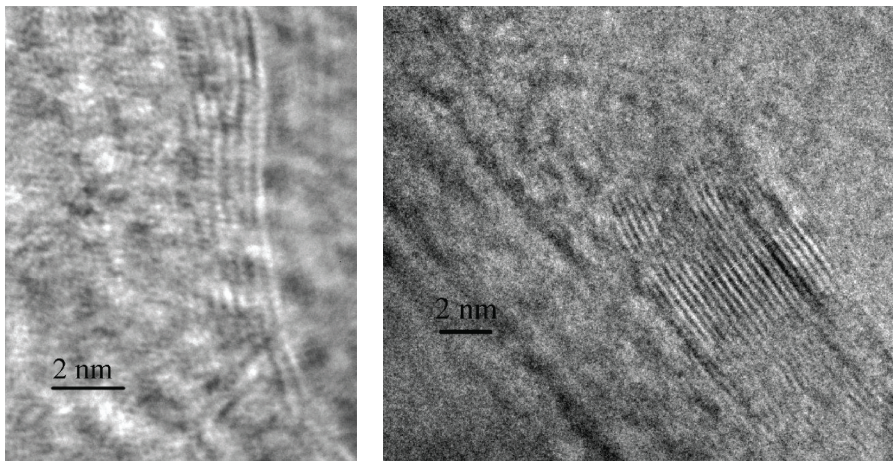

(a) (b)

Figure 3: HRTEM image of (a) BNS12 showing 6 layers of nanosheets and (b) BNS48 showing 20 layers of nanosheets. Interlayer distance was determined to be 0.33 nm.

4. Conclusions

In conclusion, we have developed a novel methodology to prepare few-layer h-BN nanosheets in high yields with acceptable purity. A 12 h reaction involving inexpensive starting reagents at moderately low temperature produced nanosheets of uniform dimension and few layers. While the morphology and crystallinity of the product were thoroughly characterized, elemental composition of the products was also determined. A detailed investigation on the variation of

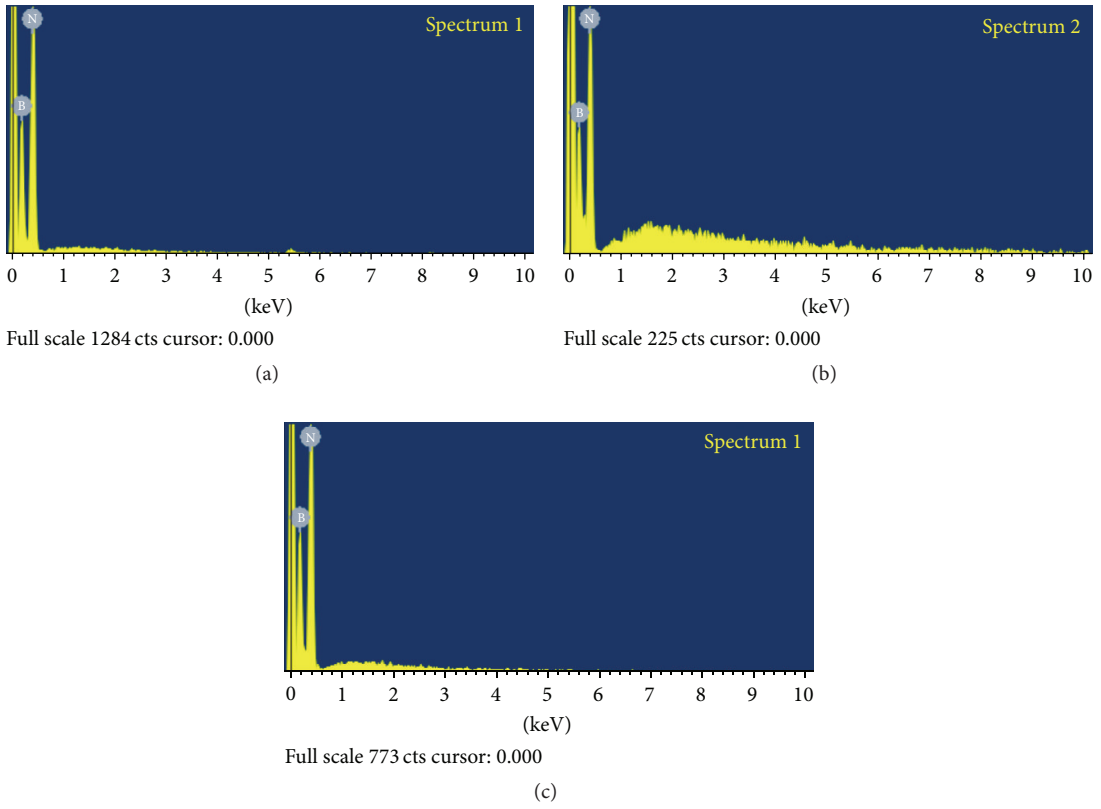

Figure 4: EDX spectra of (a) BNS12 (atomic ratio of B : N = 50.06 : 49.94); (b) BNS24 (atomic ratio of B : N = 49.9 : 50.10); and (c) BNS48 (atomic ratio of B : N = 49.66 : 50.34). No other metal impurities were found in either of the samples.

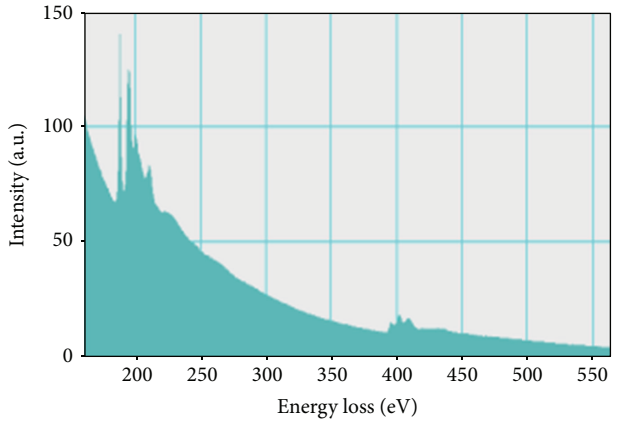

Figure 5: EEL spectrum of BNS12.

reaction temperatures and times along with the application of few-layer h-BN nanosheets for polymer composites is currently being investigated in our laboratories.

Conflict of Interests

The authors declare that there is no conflict of interests regarding the publication of this paper.

Acknowledgments

The authors gratefully acknowledge the financial support from NSF (CHE-0906179). HRTEM and EELS data were obtained from the NUANCE Facilities of Northwestern University and the authors would like to thank Dr. Shu-You Li for his help. Ms. Lori Bross is acknowledged for her timely help with low magnification TEM. Ms. Heather

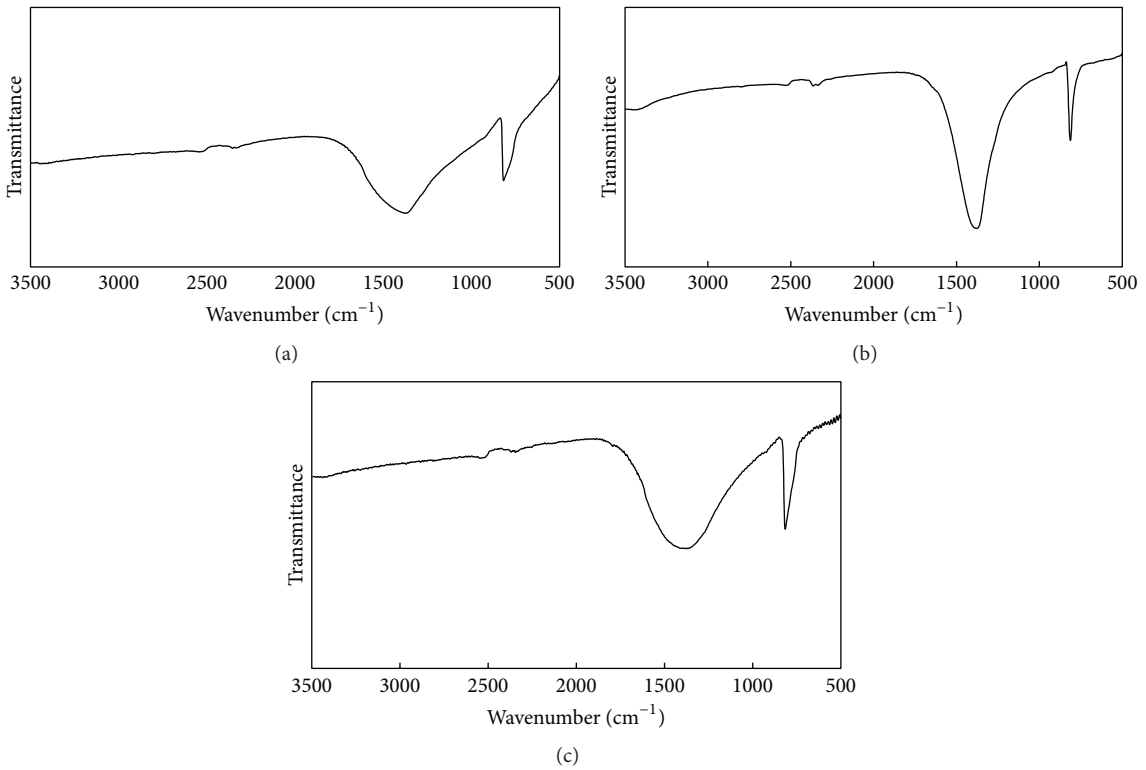

Figure 6: FTIR spectra of (a) BNS12, (b) BNS24, and (c) BNS48.

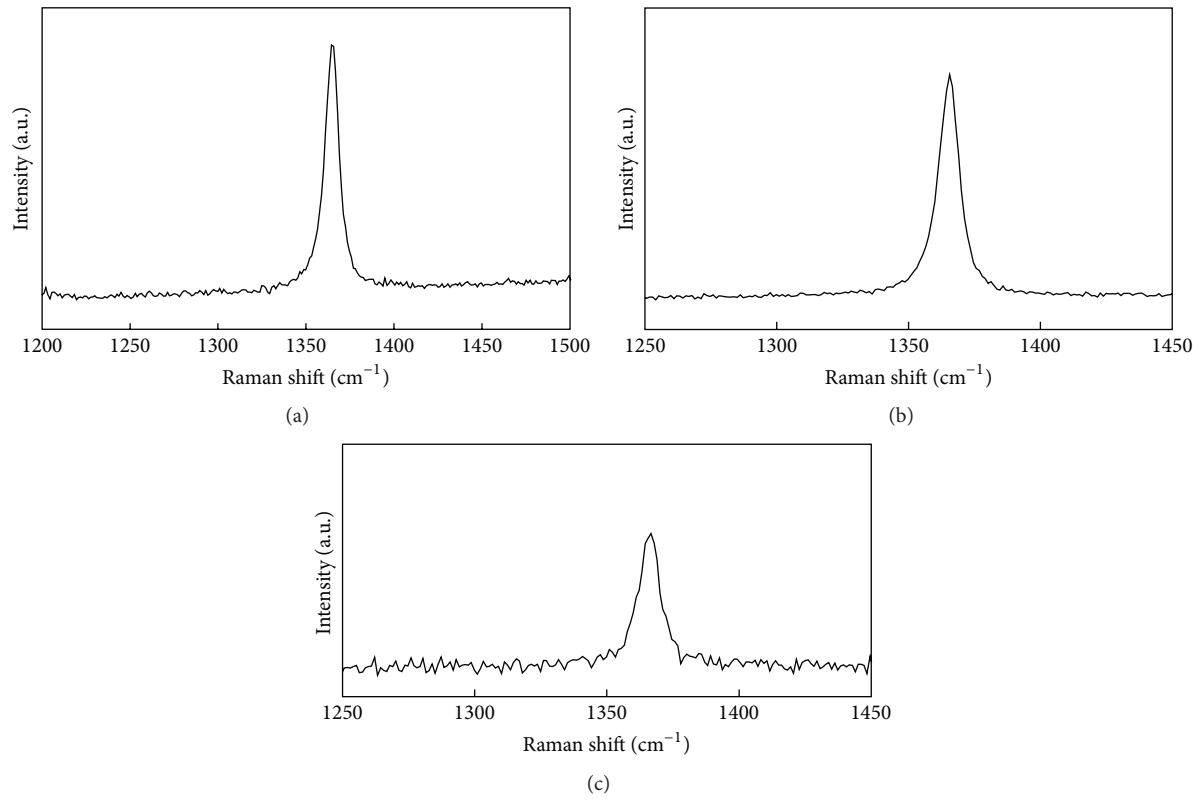

Figure 7: Raman spectra of (a) BNS12, (b) BNS24, and (c) BNS48. The spectra exhibit the Raman shift for h-BN at 1364 cm^{-1} for both BNS12 and BNS24 and 1366 cm^{-1} for BNS48, respectively.

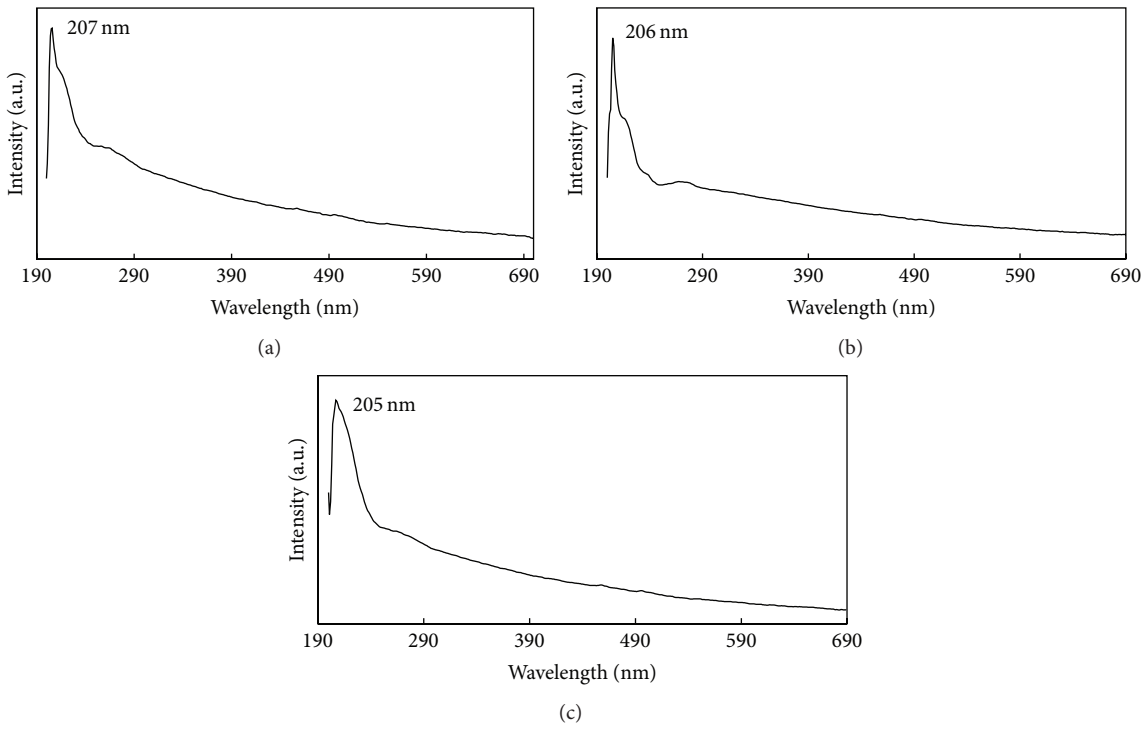

Figure 8: UV-visible spectra of (a) BNS12 with a band gap of 5.98 eV, (b) BNS24 showing the absorption band at 6.018 eV, and (c) BNS 48 exhibiting band gap of 6.048 eV.

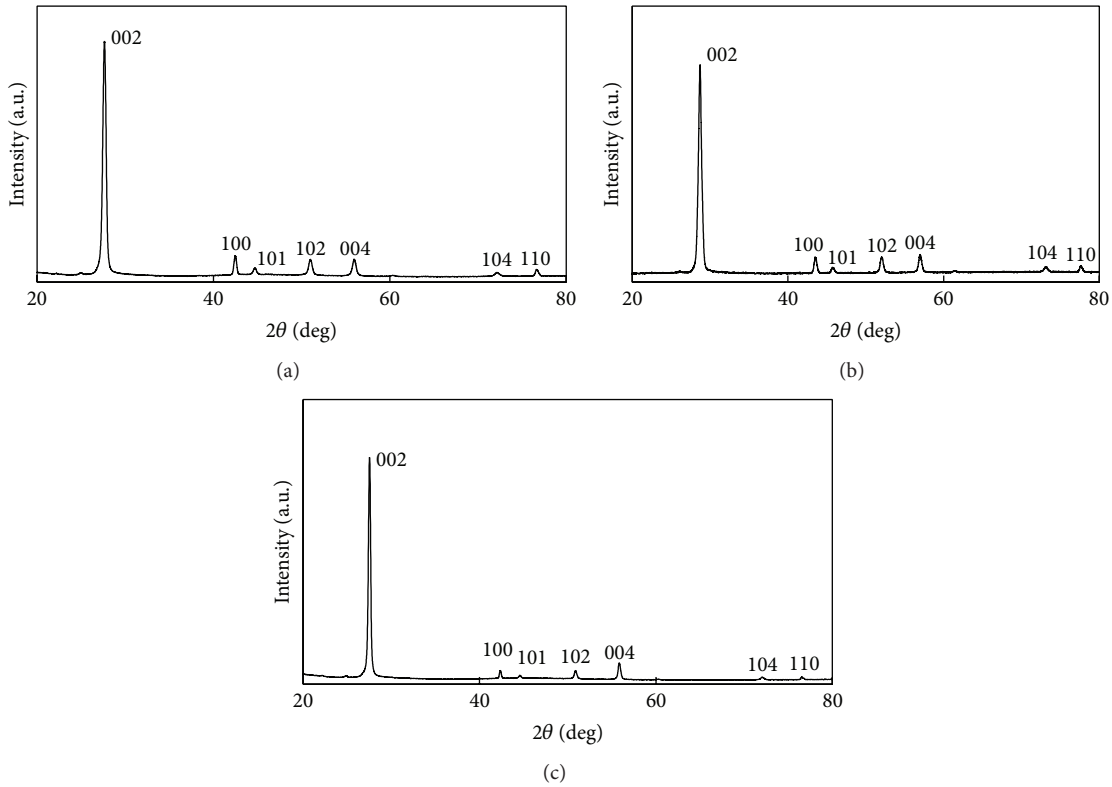

Figure 9: X-ray diffraction pattern of (a) XRD pattern of BNS12. The product synthesized at 800°C for 12 h was indexed as d_{002} = 3.225 (27.64°), d_{100} = 2.127 (42.47°), d_{101} = 2.026 (44.71°), d_{102} = 1.789 (50.98°), d_{004} = 1.642 (55.94°), d_{104} = 1.308 (72.12°), and d_{110} = 1.241 (76.68°). (b) BNS24. The product is indexed as d_{002} = 3.106 (28.72°), d_{100} = 2.077 (43.51°), d_{101} = 1.947 (45.73°), d_{102} = 1.755 (52.05°), d_{004} = 1.615 (56.98°), d_{104} = 1.294 (73.14°), and d_{110} = 1.229 (77.68°). (c) BNS48. The product is indexed as d_{002} = 3.239 (27.52°), d_{100} = 2.132 (42.34°), d_{101} = 2.031 (44.58°), d_{102} = 1.792 (50.87°), d_{004} = 1.645 (55.83°), d_{104} = 1.310 (72.01°), and d_{110} = 1.245 (76.53°).

M. Barkholtz and Mr. Karel Waska helped with SEM imaging. Raman spectroscopy of the samples was performed by Mr. Jim Hill at Reinshaw Inc. They acknowledge the help of Dr. K. Vijayaraghavan in preparing the final draft of this paper.

References

[1] A. Pakdel, X. Wang, C. Zhi et al., "Facile synthesis of vertically aligned hexagonal boron nitride nanosheets hybridized with graphitic domains," *Journal of Materials Chemistry*, vol. 22, no. 11, pp. 4818–4824, 2012.

[2] J. Duan, R. Xue, Y. Xu, and C. Sun, "Low temperature synthesis of h-BN nanoflakes," *Materials Letters*, vol. 62, no. 19, pp. 3355–3357, 2008.

[3] M. Y. Yu, D. L. Cui, K. Li et al., "Mixed nitrogen source effect in the hydrothermal synthesis of cubic BN," *Materials Letters*, vol. 61, no. 1, pp. 76–78, 2007.

[4] Z. Liu, L. Song, S. Zhao et al., "Direct growth of graphene/hexagonal boron nitride stacked layers," *Nano Letters*, vol. 11, no. 5, pp. 2032–2037, 2011.

[5] P. Sutter, R. Cortes, J. Lahiri, and E. Sutter, "Interface formation in monolayer graphene-boron nitride heterostructures," *Nano Letters*, vol. 12, no. 9, pp. 4869–4874, 2012.

[6] K. H. Lee, H.-J. Shin, J. Lee et al., "Large-scale synthesis of high-quality hexagonal boron nitride nanosheets for large-area graphene electronics," *Nano Letters*, vol. 12, no. 2, pp. 714–718, 2012.

[7] C. R. Dean, A. F. Young, I. Meric et al., "Boron nitride substrates for high-quality graphene electronics," *Nature Nanotechnology*, vol. 5, no. 10, pp. 722–726, 2010.

[8] W. Gannett, W. Regan, K. Watanabe, T. Taniguchi, M. F. Crommie, and A. Zettl, "Boron nitride substrates for high mobility chemical vapor deposited graphene," *Applied Physics Letters*, vol. 98, no. 24, Article ID 242105, 2011.

[9] J. Taha-Tijerina, T. N. Narayanan, G. Gao et al., "Electrically insulating thermal nano-oils using 2D fillers," *ACS Nano*, vol. 6, no. 2, pp. 1214–1220, 2012.

[10] T.-L. Li and S. L.-C. Hsu, "Enhanced thermal conductivity of polyimide films via a hybrid of micro- and nano-sized boron nitride," *The Journal of Physical Chemistry B*, vol. 114, no. 20, pp. 6825–6829, 2010.

[11] J. Yu, L. Qin, Y. Hao et al., "Vertically aligned boron nitride nanosheets: chemical vapor synthesis, ultraviolet light emission, and superhydrophobicity," *ACS Nano*, vol. 4, no. 1, pp. 414–422, 2010.

[12] K. Sato, H. Horibe, T. Shirai et al., "Thermally conductive composite films of hexagonal boron nitride and polyimide with affinity-enhanced interfaces," *Journal of Materials Chemistry*, vol. 20, no. 14, pp. 2749–2752, 2010.

[13] C. Harrison, S. Weaver, C. Bertelsen, E. Burgett, N. Hertel, and E. Grulke, "Polyethylene/boron nitride composites for space radiation shielding," *Journal of Applied Polymer Science*, vol. 109, no. 4, pp. 2529–2538, 2008.

[14] J. Wang, C. H. Lee, and Y. K. Yap, "Recent advancements in boron nitride nanotubes," *Nanoscale*, vol. 2, no. 10, pp. 2028–2034, 2010.

[15] Y. Lin, T. V. Williams, and J. W. Connell, "Soluble, exfoliated hexagonal boron nitride nanosheets," *The Journal of Physical Chemistry Letters*, vol. 1, no. 1, pp. 277–283, 2010.

[16] Y. Wang, Z. Shi, and J. Yin, "Boron nitride nanosheets: large-scale exfoliation in methanesulfonic acid and their composites with polybenzimidazole," *Journal of Materials Chemistry*, vol. 21, no. 30, pp. 11371–11377, 2011.

[17] Y. Xue, Q. Liu, G. He et al., "Excellent electrical conductivity of the exfoliated and fluorinated hexagonal boron nitride nanosheets," *Nanoscale Research Letters*, vol. 8, article 49, 2013.

[18] G. Cao and Y. Wang, *Nanostructures & Nanomaterials: Synthesis, Properties and Applications*, chapter 1, World Scientific Publishing, Singapore, 2nd edition, 2011.

[19] A. Ismach, H. Chou, D. A. Ferrer et al., "Toward the controlled synthesis of hexagonal boron nitride films," *ACS Nano*, vol. 6, no. 7, pp. 6378–6385, 2012.

[20] L. X. Lin, Z. H. Li, Y. Zheng, and A. S. Ahmed, "Size-dependent oriented attachment in the growth of pure and defect-free hexagonal boron nitride nanocrystals," *Nanotechnology*, vol. 22, no. 21, Article ID 215603, 2011.

[21] A. Pakdel, X. Wang, Y. Bando, and D. Golberg, "Nonwetting 'white graphene' films," *Acta Materialia*, vol. 61, no. 4, pp. 1266–1273, 2013.

[22] R. S. Pease, "An X-ray study of boron nitride," *Acta Crystallographica*, vol. 5, no. 3, pp. 356–361, 1952.

[23] C. Souche, B. Jouffrey, G. Hug, and M. Nelhiebel, "Orientation sensitive EELS-analysis of boron nitride nanometric hollow spheres," *Micron*, vol. 29, no. 6, pp. 419–424, 1998.

[24] R. Geick, C. H. Perry, and G. Rupprecht, "Normal modes in hexagonal boron nitride," *Physical Review*, vol. 146, no. 2, pp. 543–547, 1966.

[25] S. Reich, A. C. Ferrari, R. Arenal, A. Loiseau, I. Bello, and J. Robertson, "Resonant Raman scattering in cubic and hexagonal boron nitride," *Physical Review B—Condensed Matter and Materials Physics*, vol. 71, no. 20, Article ID 205201, 2005.

[26] M. H. Li, L. Q. Xu, C. H. Sun, Z. C. Ju, and Y. T. Qian, "Thermal-induced shape evolution from uniform triangular to hexagonal r-BN nanoplates," *Journal of Mateials Chemistry*, vol. 19, no. 43, pp. 8086–8091, 2009.

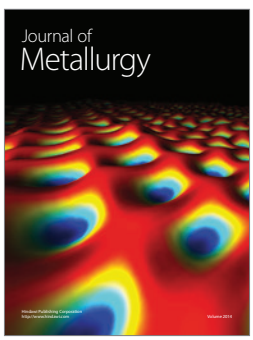

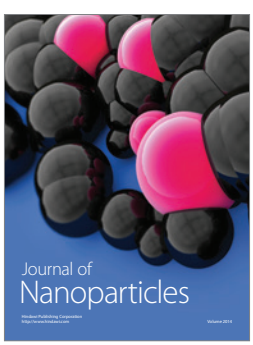

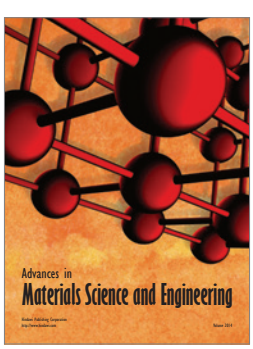

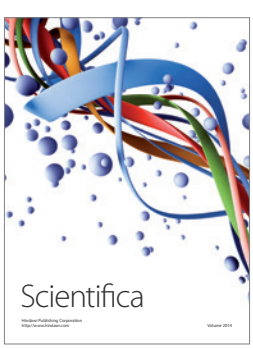

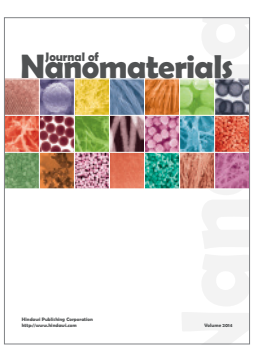

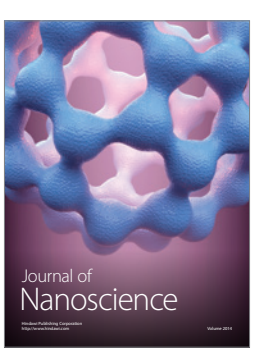

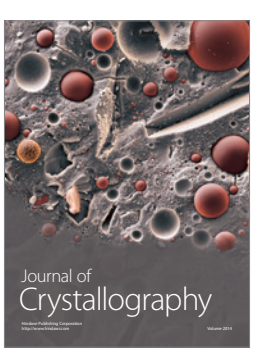

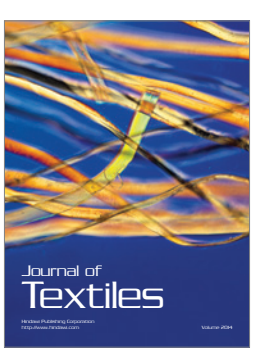

Hindawi

Submit your manuscripts at
http://www.hindawi.com